

Investigation of High-Energy Ions with High-Angle Trajectories in Hall Thruster Plumes

IEPC-2007-31

*Presented at the 30th International Electric Propulsion Conference, Florence, Italy
September 17-20, 2007*

Regina M. Sullivan*
California Institute of Technology, Pasadena, CA, 91125, U.S.A.

Paul A. Torrey†
Cornell University, Ithaca, NY, 14853, U.S.A.

and

Lee K. Johnson‡
Jet Propulsion Laboratory, Pasadena, CA, 91109, U.S.A.

Abstract: Hall thruster plume ions with high-energy, high-angle trajectories are a significant thruster integration concern. Ground tests of a BHT-200 Hall thruster (anode voltage 250 V) show that at angles greater than 60 degrees, there is a large peak in ion energy at about 30 eV with a high-energy tail, and a small but definite secondary peak at about 220 eV. An analysis of the sputtering yield energy dependence indicates that these higher energy ions have a greater impact on the total sputtering than the low energy ions. A numerical study, using a modified version of the HP-Hall code, was conducted in a first attempt at investigating this phenomenon. The HP-Hall simulations do not reveal the same phenomena as the experiment.

I. Introduction

From an integration standpoint, Hall thrusters offer a challenge because of the high-energy ions that they produce. Although most of these particles are confined to a narrow beam, those that end up at high angles off of the thruster centerline are more likely to interact with surfaces in the environment. As a consequence, wear to sensitive surfaces, as well as deposition of sputtered material in undesired locations, can result. Therefore, it is important to fully characterize those ions with high-angle trajectories.

As will be discussed, the ions that end up with these trajectories have been found to fall within a range of energies. Most of the ions are confined to low energies (below 50 eV), but a small proportion have significantly higher energies (above 100 eV), with some having energies near that of the primary beam (250 eV). Although the population of these high-energy ions is smaller, when sputtering yield is taken into account these ions can have a greater impact on surface erosion. While the low-energy ions can be accounted for by charge exchange (CEX) collisions and the mid-range-energy ions by elastic scattering [1], those ions with energies comparable to that of the main beam cannot.

* PhD Candidate, Engineering and Applied Sciences, rsulli@caltech.edu.

† Undergraduate research assistant, Applied and Engineering Physics, pat26@cornell.edu.

‡ Research Scientist, Propulsion and Thermal Engineering, Lee.K.Johnson@jpl.nasa.gov.

This study was undertaken for the purpose of characterizing the behavior these high-energy ions. Experimental methods were used to fully quantify the proportion of high-energy ions at different trajectories and determine the total sputtering yield of these ions. Additionally, modeling efforts were employed to determine whether a commonly used Hall-thruster code could replicate the results, as well as to investigate the physics underlying the generation of these ions.

II. Experimental Apparatus

In this study, a Busek BHT-200 Hall thruster, which has a nominal operating point of 250 V and 0.75 A, and which uses an external cathode, was examined. The thruster was operated in a vacuum chamber at a nominal pressure of 2×10^{-6} torr. A retarding potential analyzer (RPA) measured the energy spectrum of the thruster. The RPA was mounted on a two-axis translation stage. This stage was fixed in the vertical direction, such that the probe moved in a horizontal plane intersecting the central axis of the thruster plume.

The four-grid RPA used in this experiment was designed for use in various Hall thruster experiments. Figure 1 shows the main components of this RPA. This design employs a set of aligned molybdenum grids and a tungsten collector plate, and has an acceptance angle of 15° . The insulators are made of a commercially available plastic called Celazole. Like all RPAs, this design contains a “retarding” grid to which an increasing potential is applied. Ions with potentials above this value pass through the grid, while ions with lower potentials are rejected. An I-V curve is generated, showing the ion current admitted into the device at a given retarding potential. This is the “integrated” current, so the derivative of the data must be taken to find the potential distribution. If one then assumes that all of the ions are singly charged, then the ion energy can be found simply by multiplying the charge of the ion by its potential. However, it should be noted that this assumption is not necessarily valid for Hall thrusters [2], so in this paper will consider the ion *potential* distribution, rather than the ion *energy*, distribution generated by the RPA.

The other main components of this RPA are the “screen” and “suppressor” grids and the collector plate. The screen grid is set at a low negative voltage (~ -20 V), to reject electrons. The suppressor grid is also set at a low negative voltage (~ -20 V), to counteract secondary electron emission (SEE). Secondary electrons are generated when an ion with adequate energy collides with the collector, and if these electrons are allowed to escape cause errors in the ion current measurement. The small negative voltage helps prevent the electrons from leaving the RPA. Additionally, to further reduce SEE the collector plate is made from tungsten, a material which is resistant to SEE.

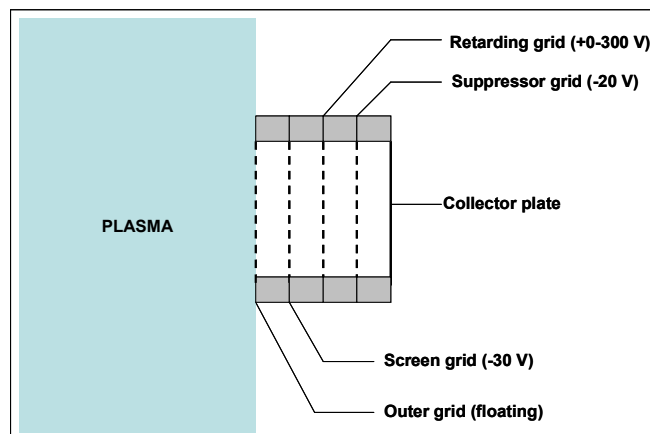


Figure 1. Schematic of RPA used in the experiment.

III. Numerical Model

A version of the HP-Hall code originally developed by J. M. Fife [3] and modified by researchers at JPL [4] was used to model the SPT-100. HP-Hall simulates the channel and near field regions of a Hall-thruster using a “hybrid-PIC” approach that employs standard particle-in-cell (PIC) methods for the ions, while using fluid equations to examine the electrons. Rather than modeling each individual ion, the code tracks the motion of clusters of ions, aptly named “superparticles” [3].

Although, the focus HP-Hall is not the thruster plume, the code was used as a starting point from which to gain insight into high-energy, high-angle ions in the plume. To examine the behavior of these ions, the code was modified in several ways. First, changes were made so that the energies of particles ending up at a certain angles off of the thruster centerline could be determined. This was done by noting the location of ion superparticles as they moved through their trajectories during the simulation, and then capturing their position, velocity, and mass after they crossed over a given boundary. These recorded superparticle crossings were then weighted proportionately by mass to obtain the total number of occurrences, which were then used to create ion energy distributions. The boundary used in this study is the one shown in Figure 2; this semi-circular surface has a radius that is 80% of the radius of the computational region to the right of the exit plane.

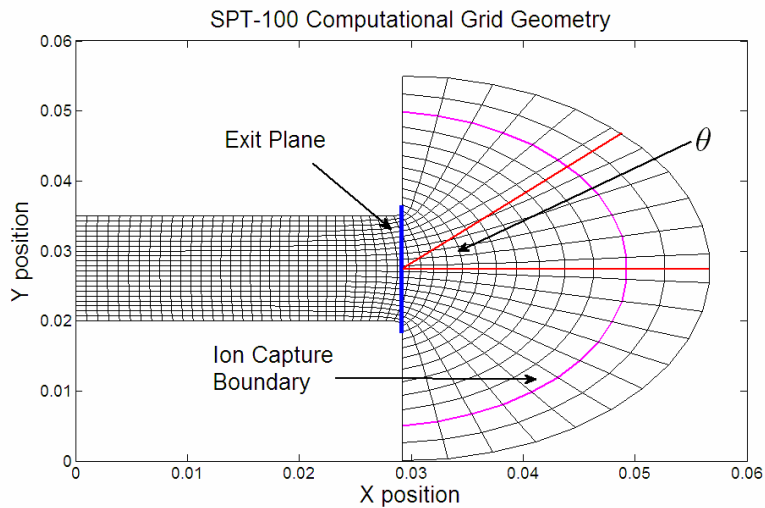


Figure 2. HP-Hall computation grid for SPT-100. Shown are the exit plane, definition of theta, and the boundary used to capture ions for determining ion energy distributions. Position is in meters.

In addition to investigating the ion energy distributions, HP-Hall was also used to examine the effect of oscillations within the potential field of the SPT-100. One possible explanation for the existence of high-angle, high-energy ions in the plume is that a high potential gradient builds up briefly and provides short periods in which ions can be progressively accelerated to high velocities. Therefore, oscillations were also studied in a rudimentary fashion using HP-Hall.

IV. Results and Discussion

A. Results from the Experiment

Figure 3 shows the ion potential spectrum produced by the RPA at different angles off of the thruster centerline. As can be seen from these plots, for angles between 60° and 75° the RPA data show a peak at approximately 30 V, with a broad tail extending from this peak, and a short peak centered at about 220 V. For angles between 75° and 90° , there is no high energy structure; only the 30 V peak is present. As mentioned previously, the lower energy structures can be accounted for by charge exchange collisions (the 30 V peak) and elastic scattering (the broad tail). However, there is no explanation readily available for the high-energy peak.

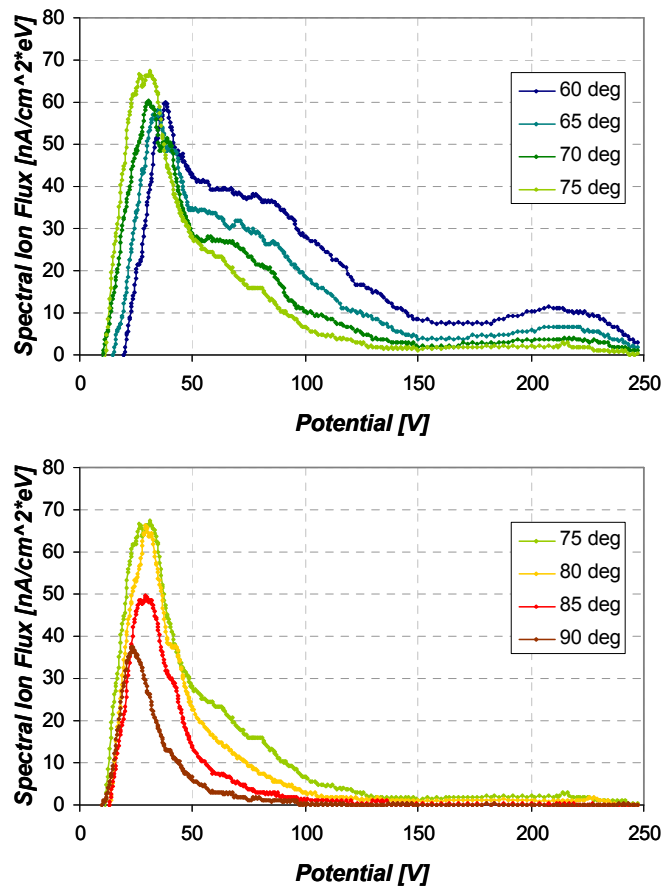


Figure 3. RPA ion potential distributions. For angles between 60° and 75° , a high-energy peak near 220 V can be seen. This peak is not present at angles above 75° .

Clearly, Figure 3 shows that the low energy peak accounts for a much greater proportion of the total plume. However, by taking sputtering yield into account, one can see that the high energy structure has a greater impact on the total sputter. Figure 5 is the result of multiplying the energy spectrum data in Figure 3 by the sputtering yield data for Molybdenum (Figure 4). As can be seen from this figure, the high energy structure makes a contribution to the total sputtering that is comparable to that of the low energy peak. This result is consistent for angles between 60° and 75° .

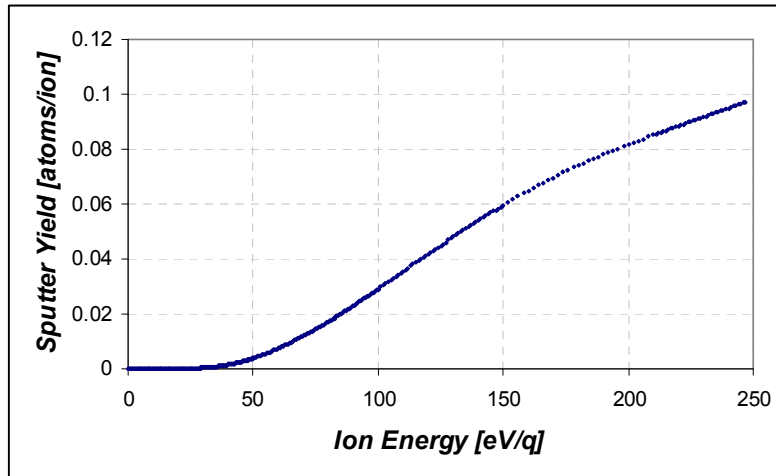


Figure 4. Sputter yield of molybdenum. Curve fit of data from experiment [5],[6].

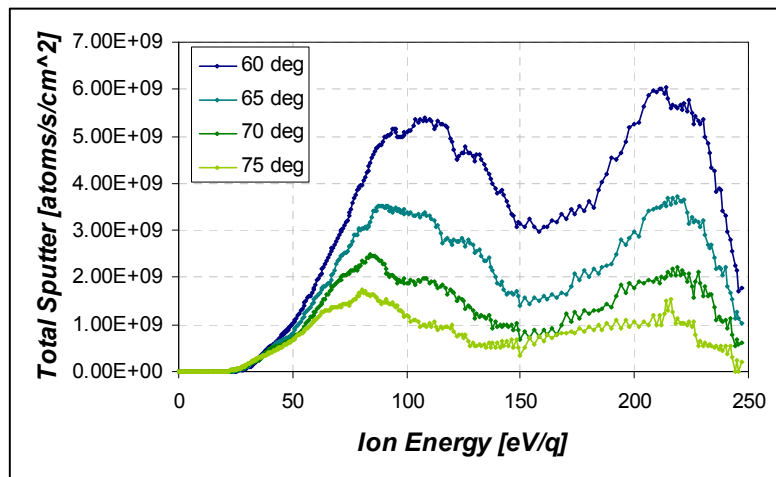


Figure 5. Total sputter yield. For angles between 60° and 75°, the contribution of the high energy peak to the total sputter is comparable to that of the low energy peak.

A. Results from the Model

1. Ion Energy Distributions

Figure 6 shows a surface plot of ion energy distribution by angle, and Figure 7 shows a contour plot of the same data. In this plot, the velocity, position, and mass data from the code were sorted into a three dimensional histogram, where the axes are ion energy, trajectory angle, and number of occurrences. A clear peak emerges at roughly 300 eV and zero radians, which is the expected energy and trajectory of the primary beam ions. There is also a coherent structure at roughly 75 eV, which can be more easily be seen in a log-scale plot of the data, as in Figure 8. This 75 eV structure appears to be evenly distributed over all angles, and roughly 1.5 orders of magnitude smaller than that of the primary beam ions. These results clearly differ from those of the experiment. As can be seen from Figures 6 and 7, at high angles there is no clear charge exchange peak near 30 eV, nor is there a high energy structure near 250 eV.

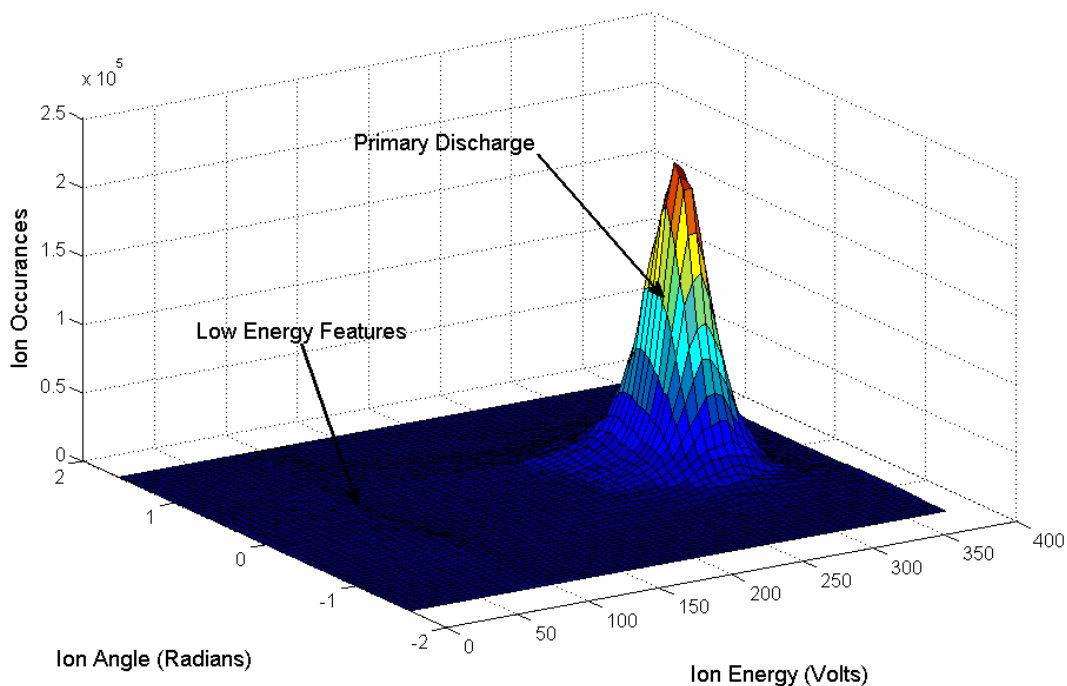


Figure 6. Surface plot of ion energy vs. ion trajectory angle. Shown here are the number of ion occurrences at a given angle from the exit plane normal direction and at a given ion energy. The 275 V primary ion discharge peak is the dominant feature, occurring at about zero radians, and the 75 volt high angle feature is also present.

Such an outcome might be expected, as the HP-Hall model does not appear to have an obvious mechanism for the generation of high-angle, high-energy ions. Figure 9 is a plot of the time-averaged plasma potential distribution in the modeled region. As can be seen from this figure, the area of high potential is contained completely within the thruster channel, and falls off rapidly outside the channel. From this potential field there is no readily apparent mechanism, such as a significant gradient perpendicular to the channel centerline, which would cause high-angle ions to be accelerated to high velocities.

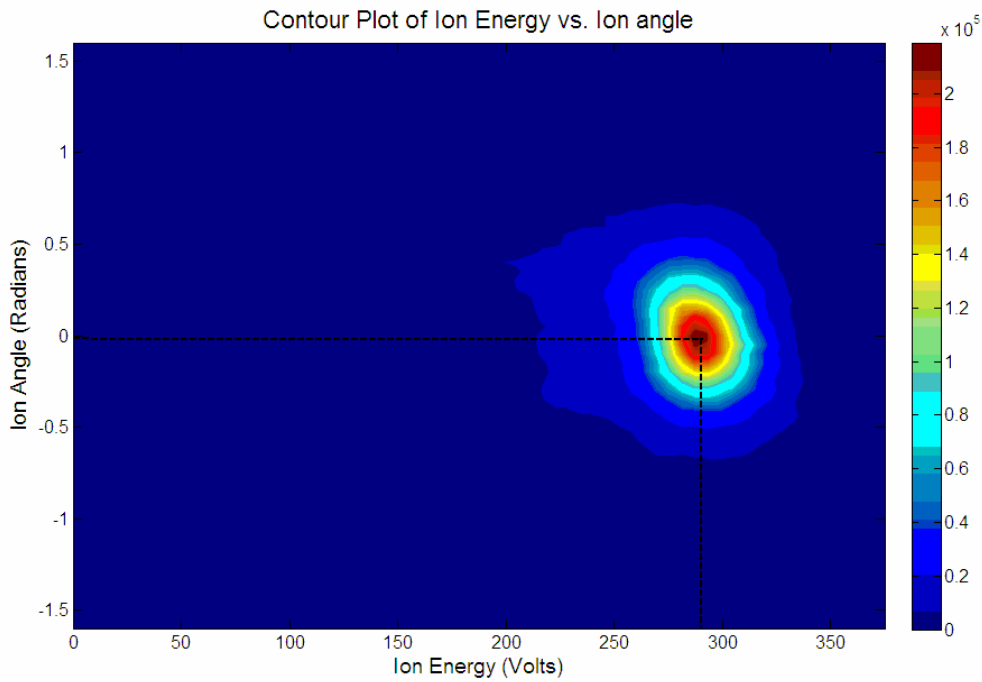


Figure 7. Contour plot of ion energy vs. ion trajectory angle. *The 275 V primary peak is clearly the dominant feature, and the 75 V structure is not discernable because of its relatively small magnitude.*

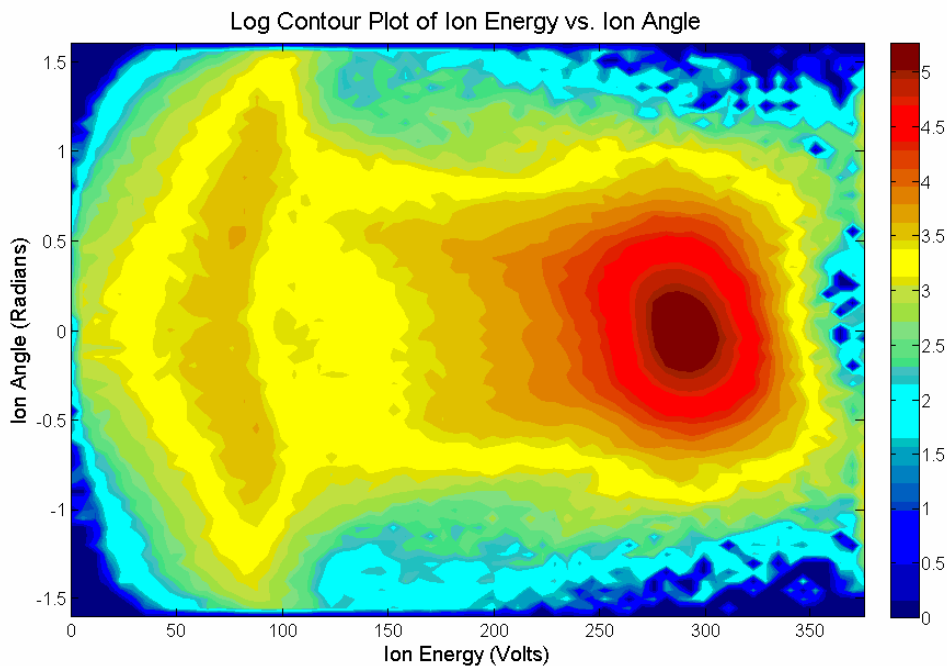


Figure 8. Log scale contour plot of ion energy vs. ion trajectory angle. *The 275 V and 75 V structures are clearly shown. Both are generally centered about zero radians and fall off smoothly at large angles. The 75 V strip is shown to maintain an approximately constant density from -1 to 1 radian.*

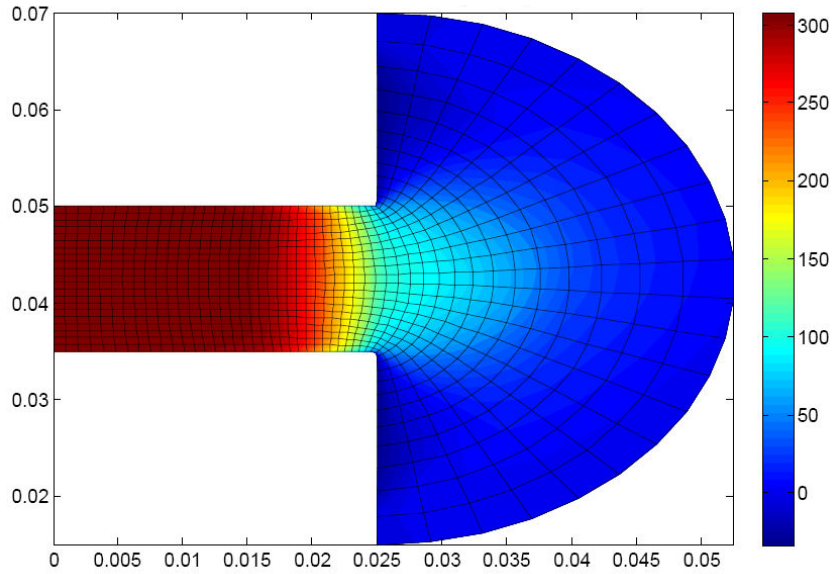


Figure 9. Time-average plasma potential. *The magnitude of the potential falls off rapidly outside the channel, and there is no significant gradient in the radial direction.*

Another revelation from the investigation of the energy distribution is that the location of the Bohm mobility transition region greatly influences the energy distribution. In general, Bohm mobility refers to an electrons ability to move across magnetic field lines through the use of a “Bohm collisional frequency” which is higher than the classically expected collisional frequency. In HP-Hall, Bohm mobility is a parameter that is essentially adjusted to achieve correct cross field transport without any physical motivation. Furthermore, the Bohm mobility coefficients used inside and outside of the acceleration zone for HP-Hall differ by significant amounts [4]. This will be discussed further in the following section.

2. Plasma Potential Oscillations

During each time step of a simulation, HP-Hall updates the plasma potential by integrating a series of electron equations [3]. Therefore, it is straightforward to plot the potential at each time step. The data in Figure 10 represent the potential field at four different times during the period of oscillation: the “start” of oscillation, one-quarter periods after start, one half periods after start, and three-quarter periods after start. The “start” time is determined by examining each frame individually and finding the frame at which the space-averaged potential has a minimum in magnitude. Similarly, the period is determined by finding the frame at which the space-averaged potential returns to a minimum in magnitude.

As can be seen from these figures, during the course of an oscillation the potential gradient is primarily axial, and as time progresses, a region of higher potential begins to extend out beyond the thruster exit plane. This causes an increase in the radial component of the gradient of the potential. This radial component has a magnitude change of about 100 V. Clearly, although this gradient could cause ions to end up at high angles, this difference is too small to create ions with energies near that of the primary beam energy, as seen in the experimental data.

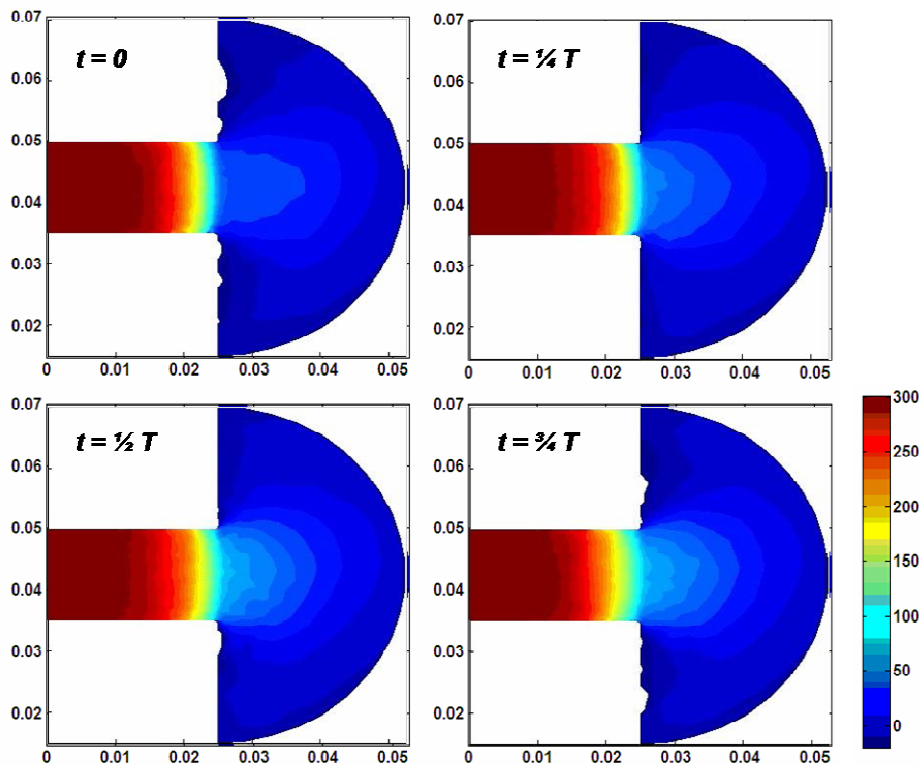


Figure 10. Plasma potential oscillations. Scale is in volts, $T = 4.5 \times 10^{-6}$. As time increases, a region of higher potential begins to extend outside of the channel. (Note: The notched areas along the edge of the field represent regions of negative potential.)

Note that Figure 10 represents a simulation using the nominal Bohm mobility, i.e. the case in which the Bohm mobility transition region starts at the exit plane and ends 2 mm to the right of the exit plane. By moving the Bohm mobility transition region forward by 2 mm (extending it further outside of the channel), one can observe notable differences in the potential field. Figure 11 shows the results of moving the Bohm mobility transition region forward by this distance. Comparing Figures 10 and 11, one can see that this change has resulted in a region of high potential that bows outward from the thruster, resulting in a radial gradient that is larger in magnitude. This magnitude is still not large enough to produce the high-energy ions seen experimentally. Nonetheless, an important conclusion from these results is that a small change in Bohm mobility can have a significant impact on the trajectories of ions as they exit the channel.

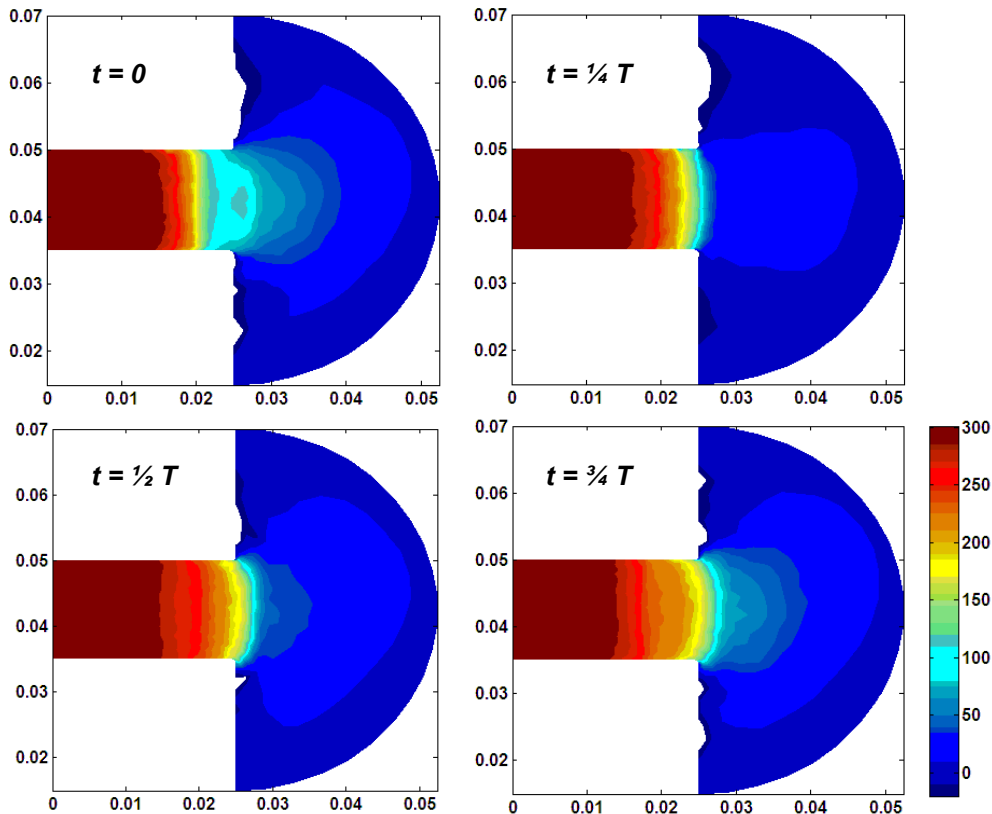


Figure 11. Plasma potential oscillations, modified Bohm mobility. Scale is in volts, $T = 4.5 \times 10^{-6}$. Bohm mobility transition region has been moved forward by 2 mm. At $t = 1/4 T$, the potential gradient is primarily axial. By the time $t = 3/4 T$, one can see that there is a gradient in the radial direction which is greater than that of the nominal case.. In this case, $T = 4.5 \times 10^{-6}$.

Conclusion

As can be seen in Figure 3, the experimental data show that a notable population of high-energy ions leaves the BHT-200 at high angles. By taking into account the sputtering yield of the ions, it is clear that those with high energy have the capability to do significant damage to any surfaces with which they collide. In contrast, the numerical data from HP-Hall do not reveal the presence of these high energy ions. Additionally, although oscillations cannot be ruled out as a possible generation mechanism for these ions, the results from this study do not provide strong evidence that these oscillations lead to the necessary conditions. Nevertheless, as shown in the numerical results, slightly modifying the location of the Bohm mobility transition region causes considerable changes in the plasma potential. Therefore, a careful review of the physics underlying electron transport should be undertaken and the results applied to HP-Hall.

It should be noted that due to the PIC approach to modeling the ions in HP-Hall, the energy distributions created by the code are less accurate than might be desired. Therefore, it might be of use to try to create a Hall thruster plume model that takes into account individual ions rather than “particles” representing thousands of ions. Efforts to create this kind of model for an ion thruster have already been carried out [6] and such a method could also be applied to a Hall thruster plume. However, to be able to correctly model these high-angle, high-energy ions, one must first understand the physical processes that generate them. Further studies should focus on this topic as well as other possible explanations for the existence of these ions.

References

- [1] Mikellides, I.G., Katz, I., Kuharski, R.A., and Mandell, M.J., "Elastic Scattering of Ions in Electrostatic Thruster Plumes," *Journal of Propulsion and Power*, Vol. 21, No. 1, 2005, pp. 111-118.
- [2] Hofer, R.R., Haas, J.M., and Gallimore, A.D., "Ion Voltage Diagnostics in the Far-Field Plume of a High-Specific Impulse Hall Thruster," *Joint Propulsion Conference and Exhibit*, 2003-4556, AIAA, Ann Arbor, MI, 2003.
- [3] Fife, J.M., "Hybrid-PIC Modeling and Electrostatic Probe Survey of Hall Thrusters," PhD Thesis, Massachusetts Institute of Technology, Sept. 1998.
- [4] Hofer, R.R., Mikellides, I.G., and Goebel, D. M., "Wall Sheath and Electron Mobility Modeling in Hybrid-PIC Hall Thruster Simulations," *Joint Propulsion Conference and Exhibit*, 2007-5267, AIAA, Cincinnati, OH, 2007.
- [5] Doerner, R. P., Whyte, D.G., Goebel, D.M., "Sputtering Yield Measurements During Low Energy Xenon Plasma Bombardment," *Journal of Applied Physics*, Vol. 93, No. 9, 2003, pp. 5816-5823.
- [6] Morris, B., "Charge-Exchange Collision Dynamics and Ion Engine Grid Geometry Optimization, PhD Thesis, California Institute of Technology, Sept. 2006.